Chapter 8
Modeling Viscoelastic Behavior in Transient Analyses

Paul Blelloch and Eric Austin

Abstract Viscoelastic materials are used extensively for vibration isolation of aerospace systems. These materials' time/frequency dependence leads to isolators with complex stiffness—and while the frequency dependence is tractable in a frequency-domain analysis, many critical simulations must be done in the time domain, where the material's time dependence is difficult to represent. The simplest approach is to assign constant isolator properties based on a single key frequency, but doing so diminishes the accuracy of the predictions over a broad frequency range.

It is possible to create a phenomenological model of the viscoelastic behavior by fitting a Maxwell model (Prony series) to test data from either a "complex stiffness" in the frequency domain or a relaxation response in the time domain. This paper shows how a generalized Maxwell model can be tuned to match complex stiffness test data for a viscoelastic isolator using a small number of parameters and then used to reproduce the frequency-dependent stiffness of the original data. In principle, constants for a Maxwell model determined in the frequency domain will also represent the relaxation behavior in the time domain. Representing general time-dependent stiffness requires one massless degree of freedom (DOF) per term in the Prony series, which requires careful treatment in a modal solution. This paper shows how to implement this technique in Nastran using residual vectors to represent the behavior of the massless DOFs and also investigates the implications of numerical integration algorithms on the accuracy of the representation in the time domain.

Keywords Damping · Viscoelastic Material · Simulation · Time Domain · Relaxation

8.1 Introduction

Viscoelastic materials are used extensively for vibration isolation in aerospace systems. One characteristic of these materials is that both the stiffness and damping are frequency dependent, so single spring/damper models are valid at only a single frequency. This becomes problematic when analysis across a broad frequency range is required. One method to address this limitation is to use frequency-dependent properties, although these can only be applied in the frequency domain and are not readily applicable in the time domain. An alternative approach is to use a simple network of linear springs and dampers, sometimes called a generalized Maxwell model, that can be tuned to match the frequency-dependent behavior of the viscoelastic isolator. These models work equally well in the frequency and time domains. We will show how a generalized Maxwell model can be tuned to match complex stiffness test data for a viscoelastic isolator using a small number of parameters and then used for time-domain analysis. Topics covered in this paper include treatment of these models in a modal analysis where retention of residual vectors and selection of an appropriate integration algorithm are critical for correctly characterizing the isolated structure behavior.

P. Blelloch (✉)
ATA Engineering Inc., San Diego, CA, USA
e-mail: paul.blelloch@ata-e.com

E. Austin
Moog CSA, Albuquerque, NM, USA
e-mail: eaustin2@moog.com

D. S. Epp (ed.), *Special Topics in Structural Dynamics & Experimental Techniques, Volume 5*, Conference Proceedings of the Society for Experimental Mechanics Series, https://doi.org/10.1007/978-3-030-47709-7_8

8.2 Phenomenological Modeling of a Viscoelastelastic Material

Viscoelastic materials are used in many aerospace applications to introduce damping into a system. As the name implies, these materials exhibit a combination of viscous and elastic responses. Creep and relaxation are two physical examples of viscoelastic behavior. Figure 8.1 shows the nature of creep, the time-dependent displacement due to a constant force f_o, and relaxation, the time-dependent force needed to enforce a constant displacement u_o. This behavior is characteristic of a "viscoelastic solid" containing elastic (k_e) in parallel with elements containing viscous stiffness k_v. Many of the explanations that follow use viscoelastic stiffness for simplicity, but all of the argument hold for a viscoelastic elastic (or shear) modulus as well.

The time dependence in creep and relaxation is due to a time-dependent stiffness, but we cannot simply relate time-dependent force and displacement by a time-dependent stiffness. However, these quantities can be related in the transform (frequency) domain via the elastic-viscoelastic correspondence principle [1]. Figure 8.2 shows the basic flow of the correspondence principle. We start in the upper left with the solution to a boundary-value problem in the time domain, ignoring the time dependence of the stiffness. Continuing clockwise, this solution is ported to the transform domain and the stiffness is then replaced with a Laplace transform of the time-dependent stiffness. This transformed stiffness is what engineers often refer to as frequency-dependent material properties. Taken a step further, the response of a viscoelastic material will have both in- and out-of-phase components of displacement with respect to a force excitation. This is the origin of the term "complex modulus" for a viscoelastic material. In theory, we could get the time response by doing the inverse Laplace transform of this solution. In practice, this is difficult and we are often satisfied with frequency response functions that capture the time-dependent viscoelastic properties.

The time-dependent responses in Fig. 8.1 are due to "creep compliance" and "relaxation stiffness." The math presented in this section describes the time-dependent force that results from a time-dependent displacement, even though engineers generally predict the opposite. Creep compliance and relaxation stiffness are related [2], so subsequent discussions refer to only the more familiar concept of stiffness.

In a phenomenological sense, the relaxation stiffness shown in Fig. 8.1 is represented by Eq. (8.1):

$$\hat{k}(t) = k_e + k_v\, e^{-t/\tau} \tag{8.1}$$

where k_e is time independent and k_e and τ characterize the exponential decay. The simple expression yields an "instantaneous" stiffness of $k_e + k_v$ at time $= 0+$ and an "equilibrium" stiffness of k_e as time gets large. For realistic materials, this would have to be generalized into a Prony series:

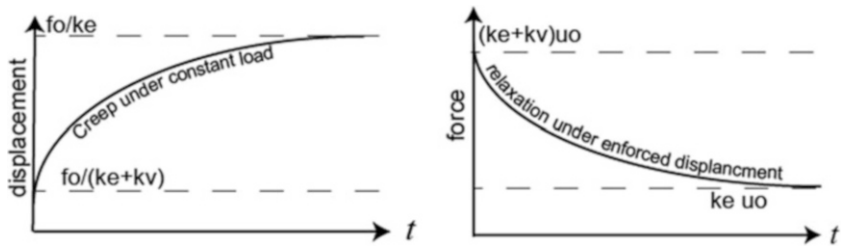

Fig. 8.1 Creep and relaxation phenomena

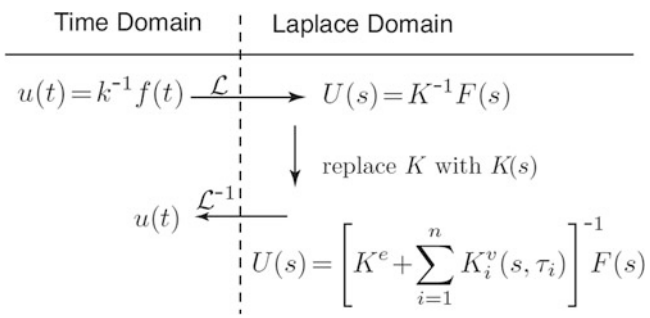

Fig. 8.2 Basic flow of the elastic-viscoelastic correspondence principle

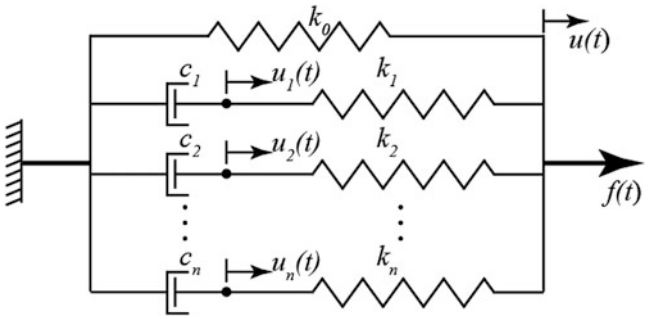

Fig. 8.3 Generalized Maxwell model for viscoelastic behavior

$$\hat{k}(t) = k_o + \sum_{i=1}^{n} k_i e^{-t/\tau_i} \tag{8.2}$$

We relate the relaxation stiffness to the actual time-dependent stiffness via the Boltzmann superposition principle [2, 3], which states that the force relaxation under an arbitrarily prescribed displacement is

$$f(t) = \int_0^t \hat{k}\,(t-\alpha)\,\frac{\partial u\,(\alpha)}{\partial \alpha} d\alpha \tag{8.3}$$

where $\hat{k}(t)$ is the relaxation stiffness. Taking the Laplace transform of Eq. (8.3) yields

$$F(s) = \left[\hat{K}(s)\right]\,[s\,U(s)] = \left[s\,\hat{K}(s)\right]\,[U(s)] = K(s)U(s) \tag{8.4}$$

Taking the Laplace transform of Eq. (8.2) and substituting into Eq. (8.4) yields

$$K(s) = s\hat{K}(s) = s\left(\frac{k_o}{s} + \sum_{i=1}^{n} \frac{k_i}{s + \frac{1}{\tau_i}}\right) = k_0 + \sum_{i=1}^{n} \frac{s\,\tau_i k_i}{1 + s\,\tau_i} \tag{8.5}$$

where k_o now denotes the elastic term, and an arbitrary number of (k_i, τ_i) terms can be used to fit actual relaxation data.

The generalized Maxwell model shown in Fig. 8.3 is a common way to model relaxation behavior in viscoelastic materials. The model has n internal DOFs that phenomenologically capture the time dependence of the material. Summing forces in the Laplace domain and eliminating the internal DOFs leads to the stiffness *K(s)* shown in Eq. (8.5) after relaxation time constants are defined as $\tau_i = c_i/k_i$.

Restate Eq. (8.5) in the frequency domain by replacing the Laplace variable s with $j\omega$, and break it into its real and imaginary components:

$$\begin{aligned} K\,(\omega) &= K(s)|_{s\to j\omega} = k_0 + \sum_{i=1}^{n} \frac{j\omega\,\tau_i k_i}{1+j\omega\,\tau_i} \\ K\,(\omega) &= k_0 + \sum_{i=1}^{n} \frac{\omega^2\,\tau_i^2 k_i}{1+\omega^2\,\tau_i^2} + j\sum_{i=1}^{n} \frac{\omega\,\tau_i k_i}{1+\omega^2\,\tau_i^2} = K'\,(\omega) + j\,K''\,(\omega) \end{aligned} \tag{8.6}$$

where K' and K'' are, respectively, the real and imaginary portions of the viscoelastic stiffness.

8.3 Converting Structural to Viscous Damping

Often the frequency-dependent behavior mild enough that the material can be approximated by a single modulus and loss factor. However, this is still problematic for time-domain integration because representing the loss factor as an imaginary stiffness matrix is not an option unless noncausal time-domain integration is considered. The relationship between structural

and viscous damping can be observed by writing the imaginary part of the stiffness for a single-DOF oscillator in the frequency domain:

$$jK'' = jC\omega \; or \; C = K''/\omega \tag{8.7}$$

A viscous damper can therefore be made equivalent to a structural damper at one frequency only. Typically, the resonant frequency is chosen for this purpose. The problem with this approach is that most practical structures have many frequencies. The traditional approach in Nastran has been to choose a single frequency (PARAM W3 or W4 depending on how the structural damping is defined) and make the equivalence at that frequency. However, the equivalent loss factor g will vary proportionally with frequency so that all modes below the chosen frequency will have lower damping and all modes above will have higher damping. An alternative approach that is available for a modally reduced system is to make the equivalence at each resonant frequency. This is done as follows:

$$\left[\hat{C}\right] = \left[\frac{1}{\sqrt{\omega_i}}\right]\left[\hat{K}''\right]\left[\frac{1}{\sqrt{\omega_i}}\right] \tag{8.8}$$

Where $\left[\frac{1}{\sqrt{\omega_i}}\right]$ is the diagonal matrix of the inverse square root of the modal frequencies ω_i, $\left[\hat{K}''\right]$ is the modally reduced imaginary stiffness matrix, and $\left[\hat{C}\right]$ is the equivalent modally reduced viscous damping matrix. Note that the diagonal elements of $\left[\hat{C}\right]$ are given as follows:

$$\left[\hat{C}\right]_{ii} = \left[\hat{K}''\right]_{ii}/\omega_i \tag{8.9}$$

So the diagonal viscous damping terms for every mode match the structural damping of that mode at the resonant frequency. This approach is only available for modal analysis and is implemented in Simcenter Nastran as PARAM, WMODAL, YES. It has proven to accurately capture structural damping when equivalent viscous damping is used, whenever modal density is sufficient high that the response is governed by resonant response.

8.4 Fitting Viscoelastic Models

While converting structural damping to viscous damping using the approach outlined in the previous section does allow for time-domain simulation of isolators modeled as lossy springs, it does nothing to capture the frequency sensitivity of the viscoelastic materials. As shown previously, viscoelasticity can be treated in either the time or frequency domain, and experimental data can also be gathered either through relaxation tests or through direct stiffness characterization in the frequency domain. The time-domain behavior is typically represented by a "master curve," which plots the relaxation modulus against a reduced time, as illustrated in Fig. 8.4 [4]. The reduced time scales to actual time based on temperature.

The equivalent in the frequency domain is a nomogram, which plots the dynamic modulus (real part of the stiffness) and loss factor (imaginary part of stiffness divided by real part) against a reduced frequency, which is again a function of temperature. A typical nomogram for a viscoelastic material is plotted in Fig. 8.5, from Lima de Sousa et al. [5].

A generalized Maxwell model can be fit to either time or frequency domain using standard numerical optimization techniques. The optimization variables are the parameters, stiffness and damping, of the generalized Maxwell model. Chae et al. [1] directly fit the time-domain relaxation data, whereas Lima de Sousa et al. [5] match the frequency-domain nomogram data. In both cases, the variables in the optimization problem are the parameters of the generalized Maxwell model (spring stiffnesses and viscous damper constants), and the objective function is a curve fit to either the time- or frequency-domain data. Note that the optimization problem is not necessarily convex, and Lima de Sousa et al. [5] use a hybrid optimization technique that first applies a genetic algorithm to find a "good" solution and then a gradient algorithm to optimize the solution. Nomogram fits for eight- and sixteen-parameter Prony terms are plotted in Fig. 8.6.

Note that nomograms are typically plotted over many orders of magnitude in frequency. Figure 8.5, for example, plots results over eleven orders of magnitude. In practice, it is typically only necessary to characterize an isolator over one to two orders of magnitude. In addition, many practical viscoelastic material isolators require metallic components to carry significant loads. These two effects result in behavior that varies less over the frequency range of interest and is easier to fit than a full nomogram.

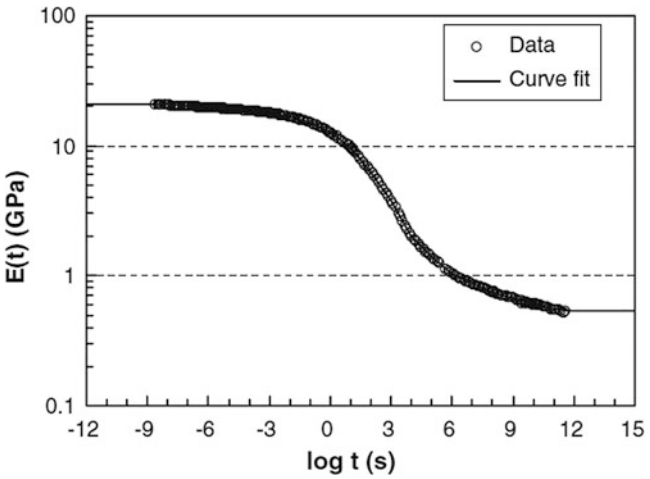

Fig. 8.4 Typical master curve for a viscoelastic material

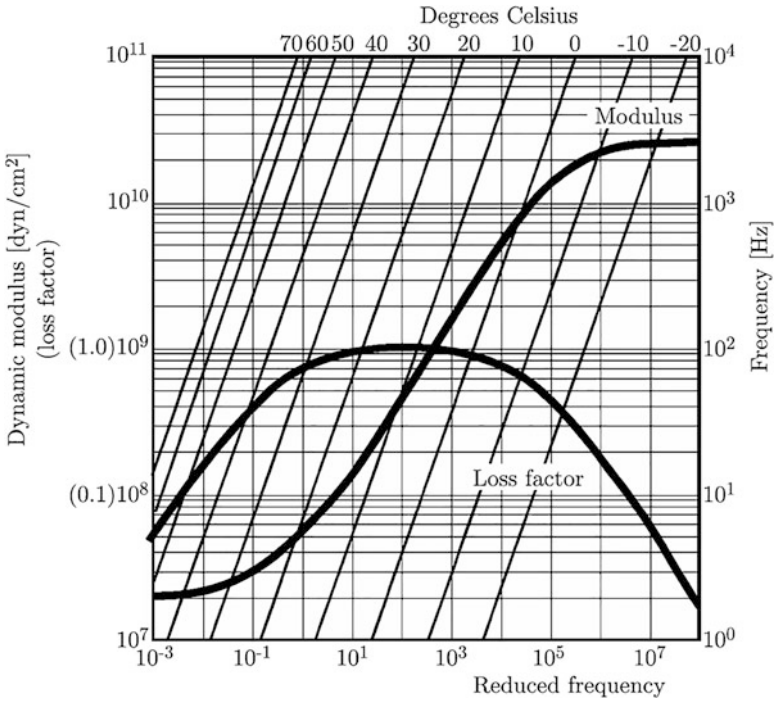

Fig. 8.5 Nomogram for EAR® C1002 [5]

8.4.1 Integrating Equations of Motion

While it is fairly straightforward to fit a generalized Maxwell model to the frequency-dependent stiffness and damping behavior of a viscoelastic material isolator, some care needs to be taken in integrating the equations of motion. This is because it is essential to accurately capture the behavior of the pseudo-DOFs to get the correct behavior. A very simple example can be used to illustrate this point. In this case, the material is EAR C-1002, described by the nomogram in Chae et al. [4]. Assuming a temperature of roughly 14 °C, the reduced frequency and actual frequency are equal. The nomogram data was digitized and a log-polynomial fit was made to get the frequency-dependent data illustrated in Fig. 8.7.

An isolator is to be designed to operate from 1 Hz to 100 Hz, which is the region denoted by the box in Fig. 8.7. A simple three-parameter Maxwell model (two springs and one damper) was fit to the data from 1 Hz to 100 Hz. The corresponding best-fit stiffness values were 7.1367E7 and 5.1641E8, and the best fit damper was 2.4022E6. The resulting fit to the modulus

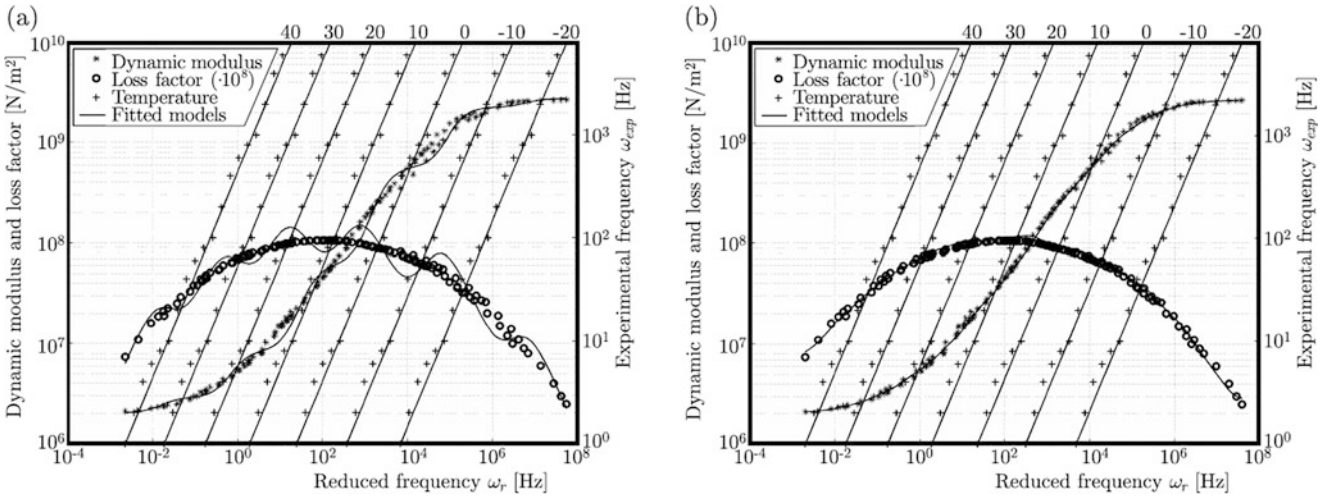

Fig. 8.6 Fits to EAR® C1002 nomogram data using 8 or 16 Prony terms [5]

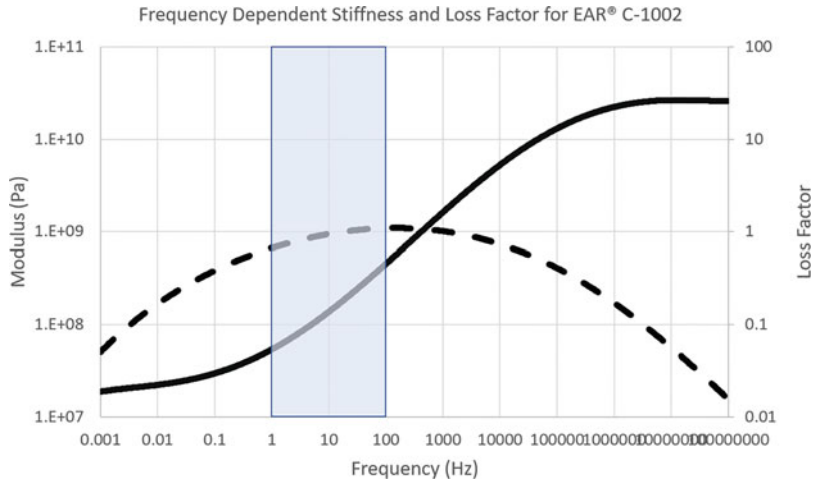

Fig. 8.7 Frequency-dependent stiffness and loss factor for EAR C-1002 at 14 °C

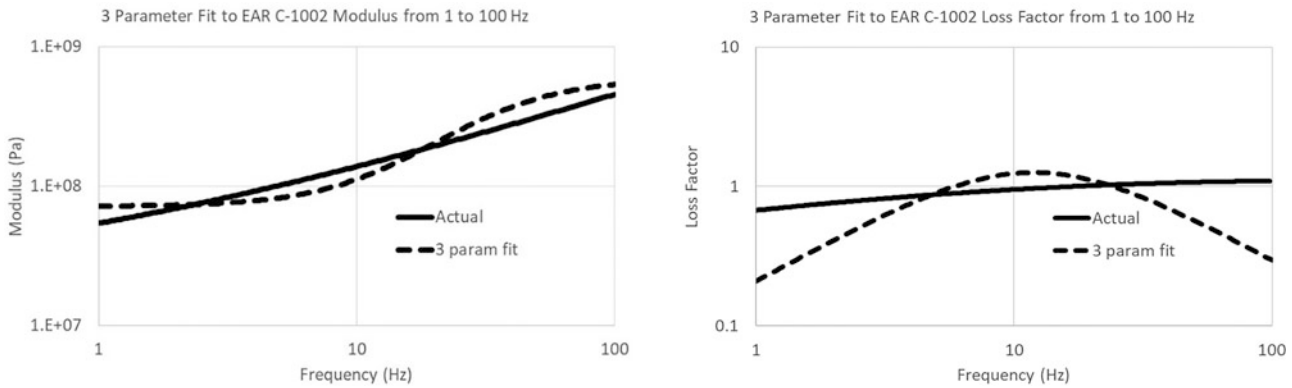

Fig. 8.8 Three-parameter fit from 1 Hz to 100 Hz

and loss factor is illustrated in Fig. 8.8. Note that the fit, particularly in loss factor, is not particularly good; however, it is sufficient for the purposes of this example.

For the purposes of this example, the stiffness and damping values were scaled down by a factor of 1E4 and a mass of 2.8352 kg was added to achieve an isolator frequency of 10 Hz. A corresponding single lossy spring model of the isolator

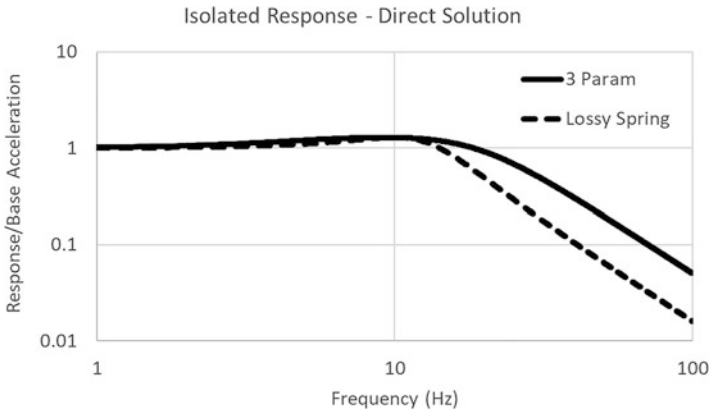

Fig. 8.9 Isolated response with three-parameter model and single lossy spring

can be calculated by looking up the stiffness and loss factor at 10 Hz. These are 1.1193E4 N/m and 1.24, respectively. Figure 8.9 illustrates the isolated acceleration of the mass for unit acceleration of the base for both the three-parameter model and the lossy spring.

Note that the lossy spring captures the resonant behavior of the isolator very accurately, but it overpredicts the isolation at 100 Hz by approximately a factor of 3. This would result in a significant error in the behavior of the isolator for an input at 100 Hz. The results in Fig. 8.9 were calculated using a direct frequency response (SEDFREQ) in Nastran, which does not require that any mass be added to the internal DOF. However, any approach based on real modes requires that a mass be added to the internal DOF such that the corresponding residual vector has a finite frequency. A mass of 1E-5 was added, corresponding to a residual mode at 11,238 Hz.[1] With this mass, the modal and direct frequency response solutions are identical in the frequency range of 1–100 Hz.

The following are the equations of motion in physical coordinates for base motion $\{x_3\}$:

$$\begin{bmatrix} 2.8352 & 0 \\ 0 & 1E-5 \end{bmatrix} \begin{Bmatrix} \ddot{x}_1 \\ \ddot{x}_{2} \end{Bmatrix} + \begin{bmatrix} 241.74 & -241.74 \\ -241.74 & 241.74 \end{bmatrix} \begin{Bmatrix} \dot{x}_1 \\ \dot{x}_2 \end{Bmatrix} + \begin{bmatrix} 6,959.3 & 0 \\ 0 & 49,859 \end{bmatrix} \begin{Bmatrix} x_1 \\ x_2 \end{Bmatrix} = \begin{Bmatrix} 6,959.3 \\ 49,859 \end{Bmatrix} \{x_3\}$$

The corresponding equations of motion in modal coordinates, using the constraint mode formulation are

$$\begin{bmatrix} 1 & 0 \\ 0 & 1 \end{bmatrix} \begin{Bmatrix} \ddot{q}_1 \\ \ddot{q}_2 \end{Bmatrix} + \begin{bmatrix} 85.2638 & -45,400 \\ -45,400 & 2.4174E7 \end{bmatrix} \begin{Bmatrix} \dot{q}_1 \\ \dot{q}_2 \end{Bmatrix} + \begin{bmatrix} 2,454.6 & 0 \\ 0 & 4.9859E9 \end{bmatrix} \begin{Bmatrix} q_1 \\ q_2 \end{Bmatrix} = \begin{Bmatrix} -1.6838 \\ -.00316 \end{Bmatrix} \{\ddot{x}_3\}$$

$$\begin{Bmatrix} x_1 \\ x_2 \end{Bmatrix} = \begin{bmatrix} 1 & 0.59389 & 0 \\ 1 & 0 & 316.23 \end{bmatrix} \begin{Bmatrix} x_3 \\ q_1 \\ q_{2.} \end{Bmatrix}$$

The challenge is now to integrate the equations with two strongly coupled, highly damped modes: one at 7.89 Hz and one at 11,238 Hz. Three different methods are considered in the following section, but first it should be noted that the coupling between the two modes is essential to capturing the behavior. The second point to note is that because of the very-high-frequency mode associated with the internal mass, any explicit integrator such as Runge-Kutta will require extremely small time steps and will therefore be very inefficient. The goal is to find an integrator that will be both stable and reasonably accurate for a model of this type. Three different integrators are considered. The first is the coupled integration algorithm implemented in Nastran, which is a variation of the implicit Newmark-beta algorithm. The second is a variation of the uncoupled integration implemented in Nastran, which puts the off-diagonal terms of the damping matrix on the right-hand side of the equations [6]. The third is a complex mode integrator, which first reduces the system to a set of uncoupled complex modes and then integrates those modes independently.

[1] In this case, a much larger internal mass could be added without significantly modifying the low-frequency dynamics, but the lower mass was chosen to provide a challenging case for time integration.

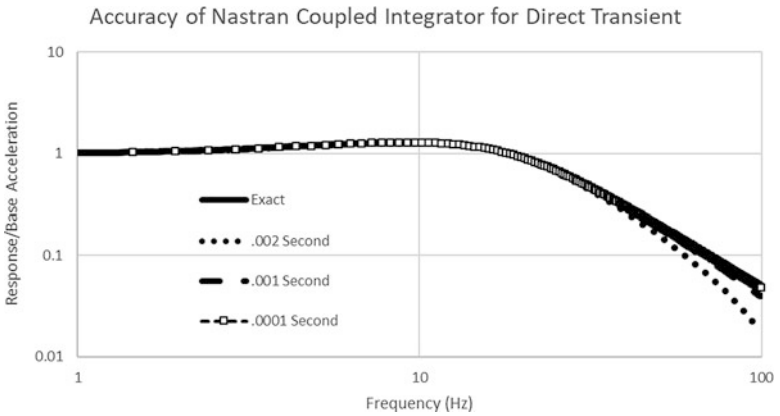

Fig. 8.10 Accuracy of Nastran coupled direct integrator for various time steps

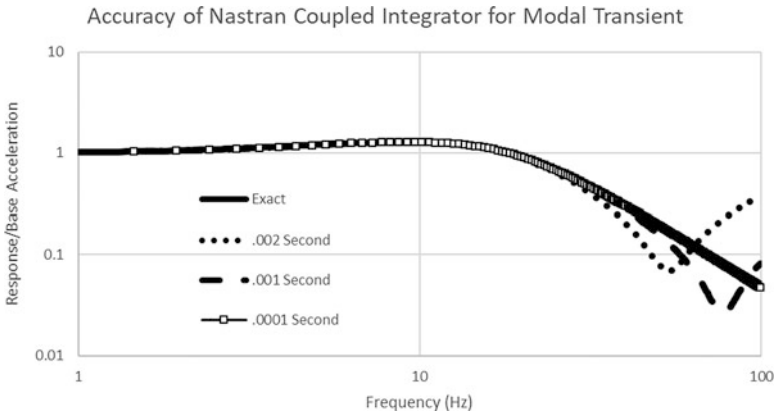

Fig. 8.11 Accuracy of Nastran coupled modal integrator for various time steps

To evaluate these algorithms, a time-domain simulation was performed for a linear sine-sweep excitation from 1 Hz to 100 Hz over a 100 s period. The data was then consistently interpolated to a 0.001 s time step, and the transfer function from input to output was then calculated using Welch's method with a Hann window, a block size of 2048 (2.048 s), and 90% overlap. The transfer functions were then compared with the "exact" three-parameter frequency domain illustrated in Fig. 8.9.

First, consider the standard Nastran coupled integrator applied without any modal reduction, with various time steps. Time steps of 0.002, 0.001 and 0.0001 s were chosen, and the results are compared with the exact solution in Fig. 8.10. The solution in this case is fairly accurate with either a time step of 0.001 s (ten time steps per highest frequency) or 0.0001 s (100 time steps per highest frequency). Accuracy falls off significantly with a time step of 0.002 s (five time steps per highest frequency).

Next, consider the accuracy of the Nastran coupled integrator applied to the modal equations of motion. The results for the same time step sizes are illustrated in Fig. 8.11. In this case, the solution with a 0.0001 s time step is still accurate, but the solutions with time steps of either 0.001 s or 0.002 s have significant errors at the higher end of the frequency range.

Next, consider the integration algorithm based on the uncoupled solution, with the off-diagonal damping elements on the right-hand side of the equations, referred to here as the Chapman algorithm [6]. The results for all three time steps for the modal solution are plotted in Fig. 8.12. In this case there is no loss of accuracy, even with the coarsest time step.

The complex mode integrator was not completed in time for this paper, although other authors have implemented this approach. It should be noted, however, that the complex roots for this set of equations are at −3.6605E1, −8.4823E1 ± 8.1459E1j, and − 2.4174E7. The root at −2.414E7 is very fast and can almost certainly be ignored, but the real root at −3.6605E1 and the complex conjugate pair at 8.4823E1 ± 8.1459E1j can almost certainly not be ignored. The application of a complex mode integrator to this problem would require handling of both real and complex conjugate roots and will not be able to assume that all roots come as complex conjugate pairs.

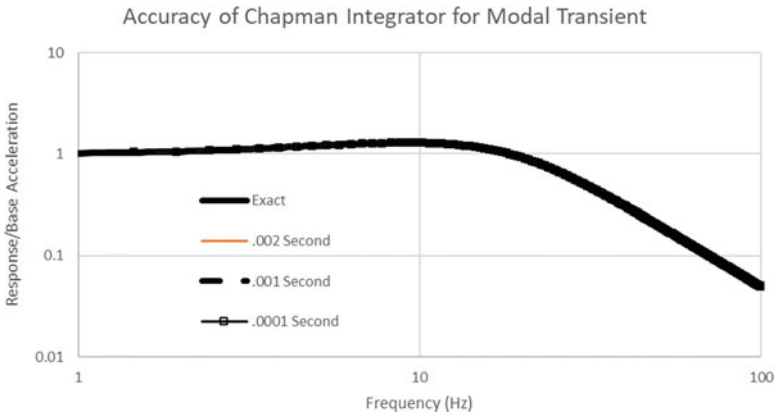

Fig. 8.12 Accuracy of Chapman modal integrator for various time steps

8.5 Summary

A method has been presented that enables simple modeling of viscoelastic isolators in the time domain. For most practical applications, a relatively small number of terms suffices and provides an excellent representation of the frequency-dependent stiffness and damping behavior. This method, however, can prove challenging with time integration of the modal equations of motion because those equations contain very high-frequency terms that must be coupled with the low-frequency modes to capture the correct isolator behavior. Explicit integrators such as Runge-Kutta are poor choices because they require very small time steps. The coupled integrator in Nastran works fairly well but should be checked for convergence with respect to time step, since results can be inaccurate even with relatively small time steps. A variation of the Nastran uncoupled integrator that puts the off-diagonal terms on the right-hand side of the equations is much more robust and gives accurate results with even relatively large time steps.

References

1. Lee, E.H.: Viscoelastic stress analysis. In: Proceedings of the First Symposium on Navel Structural Mechanics, pp. 456–482 (1960)
2. Tschoegl, N.W.: The Phenomenological Theory of Linear Viscoelastic Behavior: An Introduction. Springer-Verlag (1985)
3. Findley, W.N., Lai, J.S., Onaran, K.: Creep and Relaxation of Nonlinear Viscoelastic Materials With an Introduction to Linear Viscoelasticity. Dover (1989)
4. Chae, S.-H., Zhao, J.-H., Edwards, D.R., Ho, P.S.: Characterization of viscoelasticity of molding compounds in the time domain. J. Electron. Mater. **39**(4), (2010)
5. Lima de Sousa, T., Kanke, F., Pereira, J.T., Bavastri, C.A.: Property identification of viscoelastic solid materials in nomograms using optimization techniques. J. Theor. Appl. Mech. **55**, 1285–1297., Warsaw (2017)
6. Chapman, J.M.: Incorporating a full damping matrix in the transient analyses of nonlinear structures. In: Proceedings of Damping'93, San Francisco (1993)